🏆 reviewed paper

Is the New Silk Road Enhancing Urban Expansion? Spatio-Temporal Analysis with Remote Sensing Data

Salim Soltani, Henri Debray, Xiaoxiang Zhu, Hannes Taubenböck

(Salim Soltani, Institute for Geography and Geology, Julius-Maximilians-Universität Würzburg, Würzburg 97074, Germany, salimsoltani28@gmail.com)
(Henri Debray, German Aerospace Center, Earth Observation Center, Münchner Straße 20, 82234 Weßling, henri.debray@dlr.de)
(Prof. Dr. Xiaoxiang Zhu, German Aerospace Center, Earth Observation Center, Münchner Straße 20, 82234 Weßling; Data Science in Earth Observation, Technical University Munich, Munich, Germany; xiaoxiang.zhu@dlr.de)
(PD Dr. Hannes Taubenböck, German Aerospace Center, Earth Observation Center, Münchner Straße 20, 82234 Weßling; Institute for Geography and Geology, Julius-Maximilians-Universität Würzburg, Würzburg 97074, Germany; hannes.taubenboeck@dlr.de)

1 ABSTRACT

The world population is growing, and a majority of the population is and will be living in urban areas. Nearly 90 percent of this growth takes place in Asia and Africa. However, urbanisation processes are not distributed evenly. Mostly they are concentrated in prosperous regions, at infrastructural nodes, or along trade routes. The so-called New Silk Roads are new trade routes where massive investments are currently made to connect China with the world. The aim of this study is to analyse the dynamics of spatial urbanisation in spatial proximity to the New Silk Roads. In detail, we want to test the hypothesis whether higher spatial growth rates are recorded for cities along these routes than for cities in the same region but away from the New Silk Roads.

For this task, we apply remotely sensed data. In this study, we extracted urban areas from multitemporal Landsat data for the time period of 1990 to 2019. We classify settlements using a Random Forest (RF) supervised classification technique. We used Gray-Level Co-Occurrence Matrix (GLCM) texture features together with spectral indices as feature set. We derive training data for our classifier by a stratified sampling method using geoinformation from the Global Human Settlement Layer (GHSL) and the ESA annual Land-cover data. The resulting consistent classifications of urban areas have temporal intervals of 5 years, i.e. 1990,1995, 2000, 2005,2010,2014, 2019 and feature high accuracies.

We selected cities with over 300,000 inhabitants. We define cities in proximity to the New Silk Roads (NSR cities) within a 100 km distance vs. cities with at least 100 km distance from the NSR (non-NSR cities); these cities are located in China, central Asian countries such as Kazakhstan, including Iran, Turkey, and Russia. We quantitively analyse spatio-temporal urban expansion trends for both groups, NSR, and non-NSR cities, for testing our hypothesis. To do so, we applied various urbanisation indices such as Overall Built-up Changed Area (OBAC), Annual Expansion Area (AEA), and urban Expansion Rate (ER).

Generally, our results reveal that spatial urbanisation is increasing over the last almost 30 years in all cities among our sample. The spatial comparison of our two groups of cities reveals that our hypothesis can be confirmed: from 2014 to 2019, urban expansion in cities along the New Silk Road was significantly faster with an annual expansion rate of 339 km2 compared to 113 km2 in cities spatially distanced from the New Silk Roads. This trend did not exist before the year 2010.

Keywords: Landsat, Remote Sensing, New Silk Road, Urbanization, GHSL

2 INTRODUCTION

Urban areas have been expanding over the past decades, and it is predicted that the world population will further increase in the coming decades. According to the latest UN report on World Population Prospects (United Nations, 2019), the world population reached 7.7 billion in 2019, indicating that the global population has grown by over one billion people over the past 14 years. Sixty-one percent of the global population lives in Asia (4.7 billion), and 1.44 billion in China alone. With it, China is the world's largest country in terms of total population. In recent decades China has experienced the highest growth rates both in population and urban areas (Taubenböck et al., 2014; Shi et al., 2019) .

The Sustainable Development Goals (SDGs), particularly Goal 11 and the UN New Urban Agenda, call countries to develop National Urban Policies and strategies as an essential part of achieving economic, social, and environmental goals. Therefore, public authorities are in need of information about urban dynamics, dimensions, and forms to understand current processes and its impacts. This knowledge must be the basis to develop policy strategies for urbanisation challenges (SDGs, 2020). The most obvious change is

ISBN 978-3-9504945-0-1. Editors: M. SCHRENK, V. V: POPOVICH, P. ZEILE, P. ELISEI, C.BEYER, J. RYSER, G. STÖGLEHNER

the physical expansion of urban areas. Traditional field data collection is not viable, and conventional urban data sources are often outdated and hard to obtain (Taubenböck et al., 2009). In order to be able to map and describe this urban expansion, current, large-scale data sets are needed. Remote sensing data have become a valuable source for large-area, multi-temporal and consistent classification of settlement areas. Many studies investigated the extraction of built-up areas from medium resolution data (e.g. Doustfatemeh and Baleghi, 2016; MacLachlan et al., 2017; Verma et al., 2018). The detection of urban areas at a global scale is evolving from coarse to medium resolution open-source Earth Observation (EO) data, taking advantage of methodological and technological advances. For example, the Global Human Settlement Layer (GHSL) generated at 30m resolution (Pesaresi et al., 2016), the artificial surfaces mask of the GLOBELAND30 – GLC309 (available at 30m resolution and referring to the year 2010), (Chen et al., 2015) or at 12-meter resolution the Global Urban Footprint (GUF) (Esch et al., 2012).

Cities often developed in favorable locations. For a long time, locations on rivers or by the sea were decisive locational advantages (e.g. Kostof, 1991). The existing or future planned infrastructure is also a key locational advantage. Infrastructure nodes are one central attraction point. In general, urban areas are expected to grow further by more infrastructure development (Aljoufie et al., 2011). In 2013 the Belt and Road Initiative (BRI) was announced by the Chinese Government (Suprabha Baniya et al., 2019); this initiative is aiming at the revival of the old Silk Road, which is now referred as the New Silk Road (NSR). The planned NSR is developed based on the ancient land-based routes (Ni et al., 2017). The rise and fall of cities along the historical Silk Road are closely linked to the trade's rise and fall (Ni et al., 2017). Some studies predict that cities located along the NSR are expected to have higher growth rates due to the advancement of infrastructure connection and an expected thriving economic future (Jakóbowski et al., 2018).

Since the New Silk Road initiative's inauguration, several scientific studies related to this project have been published. However, the majority of studies explored non-urban aspects; these topics include international political economy and geopolitical economics (e.g. Lee et al., 2018; Summers, 2016; Suprabha Baniya et al., 2019), Chinese foreign policy implications (e.g. Ferdinand, 2016; Wang, 2016), the framework and assessment of the Belt and Road initiative in general (e.g. Chan, 2018; Cheng, 2016; Huang, 2016). Few studies explored aspects of urbanisation: Chen et al. (Chen et al., 2019) studied urbanisation patterns and poverty reduction on the country level for nations along the Belt and Road initiative from 1996 to 2016. Feng et al. (2017) studied spatial patterns of the urban system along the NSR using DMSP-OLS night-time light data; they analysed 273 main cities in 1992, 2003, 2014 and found that the number of relatively small cities is decreasing, and the number of large and medium-sized cities is increasing. To date, geopolitical and geo-economic aspects of the NSR have been investigated, the urbanisation aspect, however, remains mostly unexplored. In this study, we intended to investigate if spatial urban expansion along the NSR outgrows these cities far off the NSR.

2.1 Background

The ancient Silk Road was a network that connected East to West (130 B.C.- 1453 A.D.). The transportation means were camels or horses. Stops were needed for transit and food supplies. For these reasons, settlements along the Silk Road gradually became central to the trades where people and goods gather, the merchants exchanged their goods and made their transactions. These activities led to the formation of a significant number of large ancient cities along the NSR (Ni et al., 2017). The rise and fall of these ancient cities along the ancient Silk Road were closely linked to the success and fall of the trades. Thus, it is expected that the revival of the Silk Road may accelerate the expansion of the NSR cities, even the emergence of new cities. Farkhod et al. (2019) showed most of the NSR connectivity projects that are implemented and planned in the frame of the NSR projects located in central Asian countries (Table 1). These projects have been initiated to improve existing and build new infrastructure between these cities and countries, which are today only poorly linked with each other. It has been shown that transportation and economic development strongly correlate with population growth and spatial expansion of cities (Aljoufie et al., 2011). Therefore, it is expected that the NSR and its connectivity projects trigger urbanisation in the cities connected to it.

Study area

We selected all cities with over 300,000 inhabitants along the New Silk Roads (NSR cities). We defined cities within a 100 km corridor along the NSR (NSR cities) as connected to the new infrastructure

development. At the same time, we selected the same number of cities per country that are further than 100km from the NSR (non-NSR cities). We understand them as too far away for direct impact by the NSR; these cities are located in China, Kazakhstan, Kyrgyzstan, Tajikstan, Turkmenistan, Iran, Turkey, and Russia (Figure 1). We use these two groups of cities to compare urbanization rates.

Country	Projects	Total funding(mln USD)
Tajikistan	16	4515.9
Kazakhstan	14	14539.3
Kyrgyzstan	11	1773.04
Turkmenistan	5	1402.5
Uzbekistan	5	1269

Table 1. NSR projects by country (Farkhod et al., 2019)

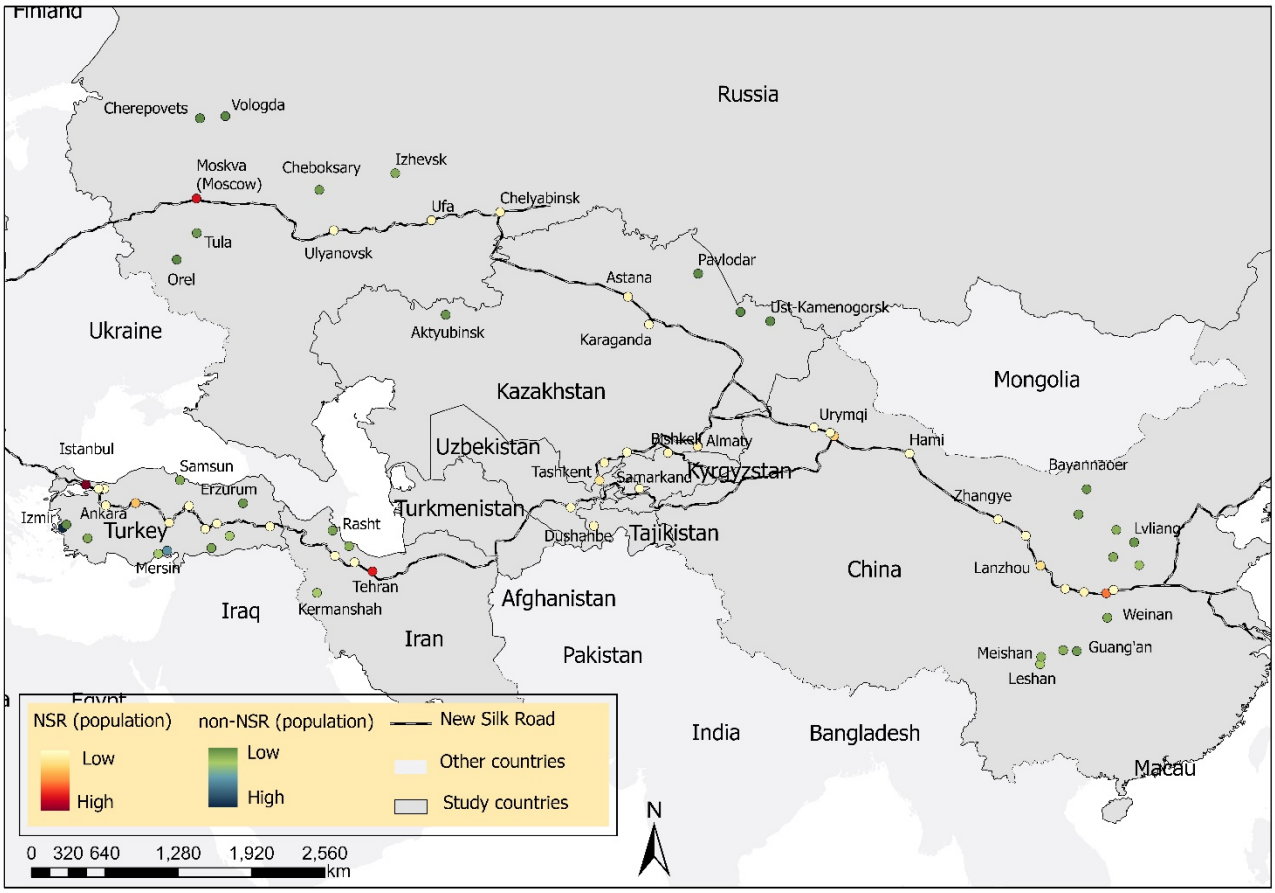

Figure 1. Geographical location of NSR and non-NSR cities

2.2 Data

For spatiotemporal analysis of urbanisation in a large study area, earth observation data proved to be an independent and cost-effective data source allowing for sufficient accuracy (e.g. Taubenböck et al., 2012). In this study, we selected – due to the need for wide area and for a 30-year temporal coverage from 1990 until today – data from the Landsat program. Data from the TM (Thematic Mapper), ETM+ (Enhanced Thematic Mapper plus), and OLI (Operational land Imager) sensors are available for our monitoring period with a comparatively high spatial resolution of 30m.

The settlement classification is performed in combination with the existing GHSL layer (Pesaresi et al., 2016), which contains a built-up area extent for 1990, 2000, 2014. We used the cloud-based platform Google Earth Engine (GEE) to process the available Landsat data. The GEE public data catalog contains an archive of multi-Petabyte of historical and present satellite imageries, especially the entire Landsat archive from Landsat-1 to Landsat-8. The GEE archive is updated every day with around 6000 new scenes from active earth observation satellite missions (Gorelick et al., 2017).

ISBN 978-3-9504945-0-1. Editors: M. SCHRENK, V. V: POPOVICH, P. ZEILE, P. ELISEI, C.BEYER, J. RYSER, G. STÖGLEHNER

3 METHODOLOGY

The developed workflow for mapping settlement areas from remote sensing data and the analysis of their spatial expansion over time included four methodological steps (Figure 2): Image-preprocessing, classification, validation and analysis of urban expansion.

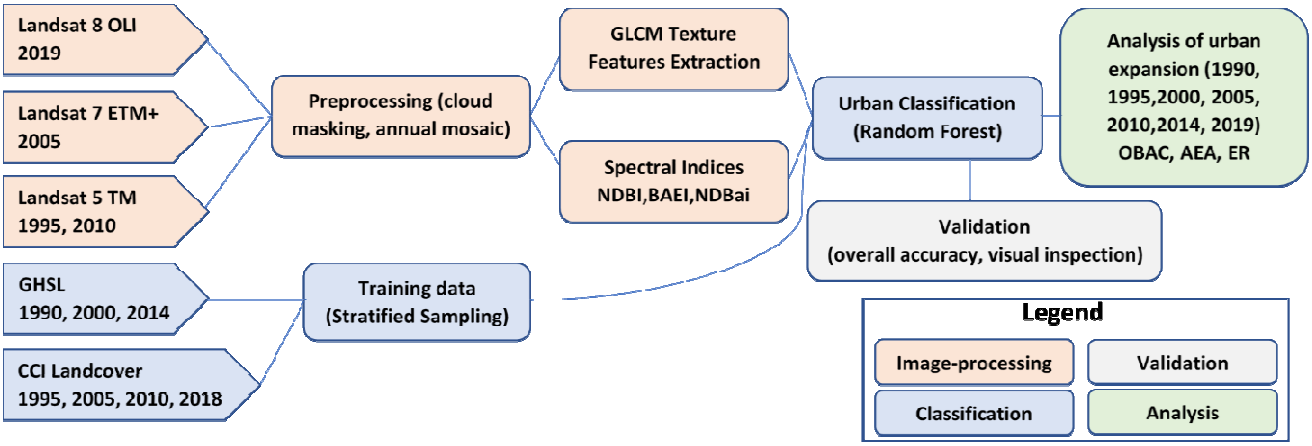

Figure 2. Overview of the methodological steps

The first step was image pre-processing, which included cleaning from cloud contamination. Surface reflectance data has been combined with a cloud mask to mask out the cloud-contaminated areas. Subsequently, annual mosaics using the median, i.e. the median value of the correspondent pixel from all available scences for the entire year have been constructed. For processing, we applied a circle buffer with 70 km diameter (equivalent to the diameter of the biggest city in the study area) around the cities' point location. In order to have a comparable spatial baseline for the cities, we applied the 'morphological urban areas' as introduced by Taubenböck et al. (2019). The morphological urban areas delineate the city from the countryside in a consistent manner along a density gradient. As this is done in a consistent manner for all cities, the spatial units are comparable, unlike historically created administrative boundaries of cities.

In a second step, we developed a feature space consisting of three GLCM texture features: variance, contrast, dissimilarity of each of the seven bands of the Landsat data. In addition, three spectral indices NDBI, BAEI, NDBai were used. These are introduced in the next section in detail. Overall, we produced a feature space with a total of 24 input variables.

The third step was classification; we generated the training data using stratified sampling from the GHSL and the ESA land-cover data as the base layer. This method takes previously produced land-cover information and returns the specified number of training points per class, considering the spatial distribution and other parameters like disproportional sample number per class area for better training data. A random forest supervised classification approach was carried out to classify the urban areas.

The fourth step was validation of the classification results; one-third of the training data were used to evaluate the overall accuracy of the RF classifier. In addition, we also investigated the results visually.

3.1 Multi-temporal land-cover classification

A land-cover classification extracting ten thematic classes (rainfed agriculture, irrigated agriculture, vegetation, forest/tree, shrubland, grassland/rangeland, bare land, water, snow, and built-up area) was performed on an individual basis, for each time step, and for each study sub-region. The main purpose of this classification was to identify urban built-up areas for the spatio-temporal measurement of urban expansion. In this study, we adopted the definition 'urban areas' as introduced by Schneider et al. (2010). This definition relates to places that are dominated by the built-up environment. The built-up environment includes all non-vegetative, human-constructed elements, such as buildings, roads, runways, etc. (a mix of human-made surfaces and materials). 'Dominated' implies coverage greater than or equal to 50% of a given landscape unit (here, the pixel). Pixels that are entirely covered by vegetation (e.g., a park) are not considered urban, even though they may function as urban space in terms of land use.

We applied the supervised random forest (Breiman, 2001) algorithm to classify urban areas. The classifier relies on the combination of texture features and spectral indices (Bramhe et al., 2018; Lu et al., 2005).

Satellite images not only contain spectral information encoded in different wavelength channels but they also feature rich information in terms of context or spatial information. To extract the urban areas effectively, the inclusion of the contextual and neighborhood information has been shown beneficial. Given that, each class or object pixels shows prominent characteristics in line with neighboring pixels. Therefore, textural image information such as the Gray-Level Co-Occurrence Matrix (GLCM) (Haralick et al., 1973) has proven meaningful for higher classification accuracy. The calculation is based on tonal (DN) differences between pairs of pixels in a spatially defined relationship with consideration of all pixel pairs within the neighborhood. Bramhe et al. (2018) reported the advantage of using Grey-Level-Co-occurrence-Matrix (GLCM) texture features together with spectral indices the extraction of built-up areas with higher accuracy. In line with this, we applied the Normalized Difference Built-up Index (NDBI), the Built-up Area Extraction Index (BAEI), and the Normalized Difference Bareness Index (NDBai). We applied the variable importance (VI) measure to optimise input variables. Based on the empirical results achieved, a total of 24 input features have been identified that contributed the most to the final result: The GLCM texture features variance, contrast, dissimilarity of each of the seven bands of the Landsat data as well as the three spectral indices NDBI, BAEI, NDBai.

We selected training data for training the classifier using a stratified sampling method (Millard and Richardson, 2015). The ESA Climate Change Initiative (CCI) (ESA, 2017) annual land-cover data were used as spatial reference for non-built-up classes. The GHLS was used for training data selection within built-up areas. The training data have been extracted separately, and the classification was run to ensure higher classification accuracy. Based on the empirical result, 2,000 training points per non-built-up land-cover class and 4,000 training points for the built-up class yielded a good result. The built-up areas' training points are further filtered with an NDVI threshold to exclude all points that have a higher value of the specified NDVI threshold to improve built-up area detection accuracy. The NDVI threshold was achieved through empirical results observing the classification accuracy.

The final classification result was then re-classified into three thematic classes: 'water', 'land', 'built-up area'. The following classes have been merged to the 'land' class; forest/tree, shrubland, grassland/rangeland, bare land, and snow. For accuracy assessment, one-third of the generated point data being independent from the trainnig data were used to evaluate the overall accuracy of the RF classifier. The accuracy assessment has been utilised for each run per study subregion.

A post-processing filter has been performed to exclude outlier pixels that were misclassified for the year 1995, 2005, 2010. The mask was taken from the GHLS layer that contains a permanent land thematic built-up class which remained stable from 1975 to 2015; this thematic class has been used to mask out few misclassified pixels to increase the classification accuracy.

3.2 Spatial units for comparison of cities

For a consistent analysis and comparison of urban spatial growth across cities, it is essential to select a suitable Urban Boundary (UB) that can correctly divide urban and rural areas (Xue et al., 2018). However, administrative units do not provide consistent units. Therefore, this unit has been shown to be inadmissible or distortions occur in comparative urban analysis (Wang et al., 2018). One suggested solution is using an UB that is generated using a harmonised and data-driven method applied for all cities. In this study, the Morphological Urban Areas (MUAs) developed by Taubenböck et al. (2019) were used as UB for further analysis. The MUAs delineate urban from rural along a decreasing built-up density from the centre to the periphery. The advantage of the MUAs are that they consistently delineate cities. Further information on the MUAs methodology can be acquired from Taubenböck et al. (2019). We calculated the extent of built-up areas in square kilometer and area-related indices for all cities based on the respective UB.

3.3 Measuring physical expansion of cities

The higher-ranking goal of this study was to test whether spatio-temporal expansion of NSR cities is higher than in non-NSR cities. To do so, we applied urbanisation indices. Urbanisation indices are used to measure the extent and speed of urbanisation over time. We used three indices: The Overall Built-up Changed Area (OBAC) measures the amount of changed built-up area between two-time steps, the Annual Expansion Area (AEA) measures the amount of annual urban expansion, and the urban Expansion Rate (ER) index is used as

ISBN 978-3-9504945-0-1. Editors: M. SCHRENK, V. V: POPOVICH, P. ZEILE, P. ELISEI, C.BEYER, J. RYSER, G. STÖGLEHNER

an indicator of urbanisation speed (Qian and Wu, 2019; Haas, 2016). The formulas of the three indices are introduced below.

Overall Built-up changed Area OBCA = BA (t2) - BA (t1) (1)

Annual Expansion Area AEA = [BA (t2) - BA (t1)]/(t2 - t1) (2)

Expansion Rate ER = ([BA (t2) - BA (t1)]/ BA(t1))*100 (3)

BA stands for the built-up area, BA(t) refers to the amount of settlement areas in particular time steps. The letter (t) refers to the time, and t1 is the prior time of t2.

3.4 Results: Spatio-Temporal Analysis of Urbanization along and off the New Silk Road

In general, we measured cities along the New Silk Road with higher urban growth rates than cities spatially off the route. This result confirms our central hypothesis.

Figure 3 illustrates the spatio-temporal evolution of settlement patterns from 1990 until 2019 for the examples of Almaty (Kazakhstan) and Kermanshah (Iran). Almaty is a city along the NSR, and Kermanshah is a sample city off the NSR by our definition. In addition, the morphological urban areas are shown in the figure to encompass the main settlement. The figure shows urban growth in general, but it is particularly interesting to see how growth in Kermanshah occurs along linear structures.

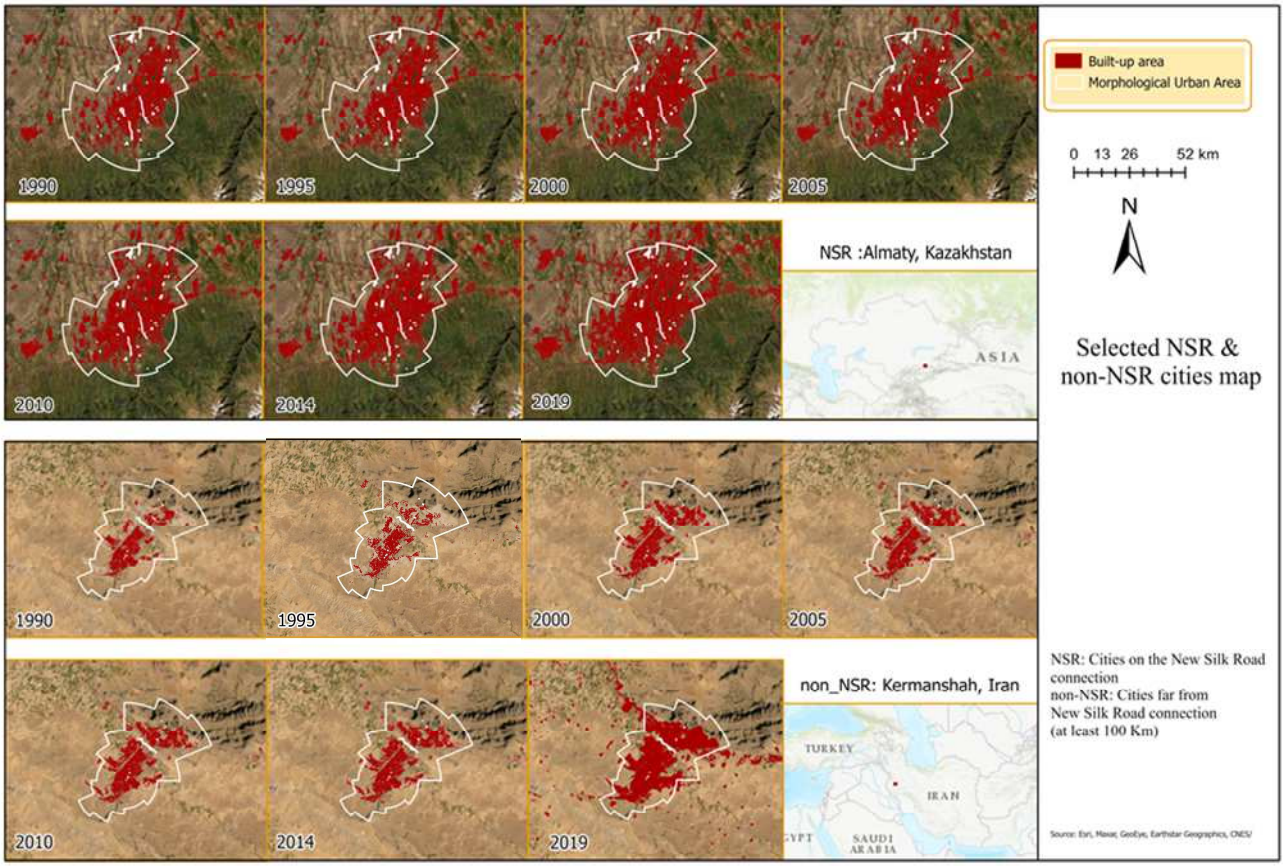

Figure 3. Classification result for NSR and non-NSR studies

We have evaluated the classification accuracy during the classification process; we used one-third of the training sample to evaluate the classifier's performance, while the remaining two-thirds were used to train the classifier. We measured the overall accuracies range from 75% to over 90 % dependeding on the particular city.

We have calculated the total urban area in square kilometers of all cities for each period, and we have calculated the area-related urban indices (OBAC, AEA, ER) to measure and quantify the magnitude of urban expansion in NSR and non-NSR cities. The total built-up area for the NSR cities detected in the initial year of our study 1990 was 4230.93 km2. We measured an increase to a total built-up area of 7926.06 km2 in 2019. In contrast, the total built-up area for the non-NSR cities was 1154.77 km2 in 1990 and then increased to 2919.52 km2 in 2019.

To investigate further the degree of change in both groups of cities, the three utilised urbanisation indices are calculated and they are as follows: The OBCA index, which shows the changed built-up area at two-time steps, and the AEA, which shows the annual expansion area, reveal that there has been generally fluctuating urban growth rates over the five year or yearly time periods. However, what is particularly interesting here is that from 2014 onwards, i.e. after the New Silk Road was launched as a project, the absolute area growth of the cities has been measured highest by far (Table 1).

year	1990-1995	1995-2000	2000-2005	2005-2010	2010-2014	2014-2019
NSR cities	1026 (205)	223 (45)	333 (67)	232 (46)	185 (46)	1696 (339)
Non-NSR cities	654 (131)	80 (16)	253 (51)	155 (31)	60 (15)	563 (113)

Table 2: Overall Built-up Changed Area (OBCA) and Annual Expansion Area (AEA) in km² (rounded)

For a relative analysis, we calculated the ER, which is used to capture the speed of urbanisation for the study periods. The ER compares the amount of urban land of two-time steps as a relative measure of urbanisation speed. The results of the ER index show that NSR cities expanded compared to non-NSR cities at a relatively slower speed from 1990 to 2010. However, we measured from 2010 onwards that the expansion speed of NSR cities overtakes the non-NSR cities (Table 3).

year	1990-1995	1995-2000	2000-2005	2005-2010	2010-2014	2014-2019
NSR	24.25	4.25	6.08	3.99	3.06	27.22
Non-NSR	56.64	4.40	13.40	7.24	2.61	23.90

Table 3: Expansion Rate (ER) in percent

Overall, we found that spatial urbanisation significantly increased from the years 2010 and onwards, independent whether cities are along the New Silk Road or not. At the same time, the analysis showed that urban expansion along the New Silk Road accelerated in the last decade. While until 2010 growth rates were actually slightly higher in non-NSR cities, we see that from 2010 NSR cities have higher growth rates.

4 DISCUSSION

It is interesting to see, that our main finding, that urban expansion is from 2010 onwards higher in NSR cities than far off the New Silk Roads, coincides with the inauguration of the NSR. However, we must clarify that our analysis is only descriptive and shows an effect that demonstrates a possible consequence of investments along the trade route. But, we cannot establish a clear causal relationship here due to the data situation as well as due to the manifold possible influencing factors.

This increase of urbanisation rates in the last decade coincides with the inauguration of the NSR. After the announcement of the BRI initiative, many projects were implemented to build as well as to reinforce the necessary transportation infrastructure to connect NSR cities and to ultimately connect China and the participating countries to Europe. It is well accepted that new economic opportunities in the cities attract more urban dwellers and consequently result in the expansion of cities. Based on the result achieved in this study, the result indicates an increased growth of built-up areas in NSR cities. Thus, there appears to be a link to increased urban growth rates.

With respect to our input data, we have measured an overall high accuracy of classification results. However, the effects of misclassifications to our results must remain unclear here. In addition, we measured for the period from 1990-1995 very high growth rates for all three urban indices. These are related to methodological differences, where higher settlement detection rates were performed in 1995 compared to 1990 due to an improved data situation. Thus, we assume growth rates from 1990 to 1995 overestimated in our analysis. From 1995 onwards, however, results are consistent and plausible. Beyond, by the applied method in this study some challenges in mountainous regions were observed; the geological structures and terraces similar in spectral reflectance to settlements were also included as built-up areas. Their effect, however, was low as these misclassified pixels were mostly excluded using the morphological urban areas in the final analysis.

5 CONCLUSION

In this paper, we have investigated the spatial urbanisation trend in cities along the NSR in comparison to cities off the NSR. We found that, indeed, NSR cities feature increased urbanisation rates since 2010 and

ISBN 978-3-9504945-0-1. Editors: M. SCHRENK, V. V: POPOVICH, P. ZEILE, P. ELISEI, C.BEYER, J. RYSER, G. STÖGLEHNER

higher urbanisation rates than cities spatially not directly connected to the NSR. Beyond, the results of the analysis confirm the accelerated growth cities in the study region in the recent decade in general. Although we cannot establish a causal relationship here, the NSR initative with its developed projects seems to trigger these expansion rates.

Remote sensing proved to be a reliable tool for large-scale analysis of urbanisation trends. The proposed method of extracting urban areas using medium resolution multitemporal Landsat data resulted in acceptable classification accuracies. In linking these spatial data with other data on economic, demographic, social or environmental issues, we see a high potential for new scientific insights along such a megaproject. Beyond, from a remote sensing point of view, we encourage further research with higher resolved satellite data to investigate this topic more in-depth. As the New Silk Roads will expand beyond our study areas, further studies are encouraged systematise and confirm the identified trends.

6 REFERENCES

Aljoufie, M., Zuidgeest, M., Brussel, M., & van Maarseveen, M. (2011). Urban growth and transport: understanding the spatial temporal relationship. In A. Pratelli, & C.A. Brebbia (Eds.), Urban Transport XVII (pp. 315–328): WIT PressSouthampton, UK.

Bramhe, V.S., Ghosh, S.K., & Garg, P.K. (2018). EXTRACTION OF BUILT-UP AREA BY COMBINING TEXTURAL FEATURES AND SPECTRAL INDICES FROM LANDSAT-8 MULTISPECTRAL IMAGE. ISPRS - International Archives of the Photogrammetry, Remote Sensing and Spatial Information Sciences, XLII-5, 727–733.

Breiman, L. (2001). Random Forests. Machine Learning, 45, 5–32.

Chen, J., Chen, J., Liao, A., Cao, X., Chen, L., Chen, X., He, C., Han, G., Peng, S., Lu, M., Zhang, W., Tong, X., & Mills, J. (2015). Global land cover mapping at 30m resolution: A POK-based operational approach. ISPRS Journal of Photogrammetry and Remote Sensing, 103, 7–27.

Doustfatemeh, I., & Baleghi, Y. (2016). Comprehensive urban area extraction from multispectral medium spatial resolution remote-sensing imagery based on a novel structural feature. International Journal of Remote Sensing, 37, 4225–4242.

ESA (2017). Land Cover CCI Product User Guide Version 2. Tech. Rep. Available at: maps.elie.ucl.ac.be/CCI/viewer/download/ESACCI-LC-Ph2-PUGv2_2.0.pdf.

Esch, T., Taubenböck, H., Roth, A., Heldens, W., Felbier, A., Thiel, M., Schmidt, M., Müller, A., & Dech, S. (2012). TanDEM-X mission–new perspectives for the inventory and monitoring of global settlement patterns. Journal of Applied Remote Sensing, 6. https://www.spiedigitallibrary.org/journals/journal-of-applied-remote-sensing/volume-6/issue-1/061702/tandem-x-mission-new-perspectives-for-the-inventory-and-monitoring/10.1117/1.jrs.6.061702.short.

Farkhod, A., Alina, A., Anna, A., Bahtiyor Eshchanov, Daniyar, M., Indra Overland, & Roman, V. (2019). BRI in Central Asia: Rail and Road Connectivity Projects, https://papers.ssrn.com/sol3/papers.cfm?abstract_id=3505258.

Feng, J., Bai, L., wang, K., Zhang, X., Xie, N., Ran, Q., Guo, M., & Xu, L. (2017). Analysis of Spatial Pattern of Urban System along the Overland Silk Road Economic Belt Using DMSP-OLS Nighttime Light Data. IOP Conference Series: Earth and Environmental Science, 57, 12052.

Ferdinand, P. (2016). Westward ho-the China dream and 'one belt, one road': Chinese foreign policy under Xi Jinping. International Affairs, 92, 941–957.

Gorelick, N., Hancher, M., Dixon, M., Ilyushchenko, S., Thau, D., & Moore, R. (2017). Google Earth Engine: Planetary-scale geospatial analysis for everyone. Remote Sensing of Environment, 202, 18–27.

Huang, Y. (2016). Understanding China's Belt & Road Initiative: Motivation, framework and assessment. China Economic Review, 40, 314–321.

Jakóbowski, J., Kaczmarski, M., Popławski, K., & Klimowicz, M. (2018). Kolejowy jedwabny szlak. Połączenie kolejowe UE-Chiny uwarunkowania, aktorzy, interesy. Warszawa: Ośrodek Studiów Wschodnich im. Marka Karpia.

Haas, J. (2016). Remote Sensing of Urbanization and Environmental Impacts. Doctoral Thesis in Geoinformatics.

Kostof, S. (1991). The city shaped. Urban patterns and meanings through history / Spiro Kostof ; original drawings by Richard Tobias. London: Thames and Hudson.

Lee, S.-O., Wainwright, J., & Glassman, J. (2018). Geopolitical economy and the production of territory: The case of US–China geopolitical-economic competition in Asia. Environment and Planning A: Economy and Space, 50, 416–436.

Lu, D. & Weng Q. (2005). Urban Classification Using Full Spectral Information of Landsat ETM&#x01; Imagery in Marion County, Indiana.

MacLachlan, A., Roberts, G., Biggs, E., & Boruff, B. (2017). Subpixel land-cover classification for improved urban area estimates using Landsat. International Journal of Remote Sensing, 38, 5763–5792.

Millard, K., & Richardson, M. (2015). On the Importance of Training Data Sample Selection in Random Forest Image Classification: A Case Study in Peatland Ecosystem Mapping. Remote Sensing, 7, 8489–8515.

Ni, P., Kamiya, M., & Ding, R. (2017). Cities Network Along the Silk Road. Singapore: Springer Singapore.

Pesaresi, M., Daniele Ehrlich, Stefano Ferri, Aneta Florczyk, Sergio Freire, Matina Halkia, Andreea Julea, Thomas Kemper, Pierre Soille, & and Vasileios Syrris. (2016). Operating procedure for the production of the global human settlement layer from Landsat data of the epochs 1975, 1990, 2000, and 2014. Luxembourg: Publications Office.

Qian, Y., & Wu, Z. (2019). Study on Urban Expansion Using the Spatial and Temporal Dynamic Changes in the Impervious Surface in Nanjing. Sustainability, 11, 933.

Haralick, R. M., Shanmugam, K., & Dinstein I. (1973). Textural Features for Image Classification. IEEE Transactions on Systems, Man, and Cybernetics, SMC-3, 610–621.

Schneider, A., Friedl, M.A., & Potere, D. (2010). Mapping global urban areas using MODIS 500-m data: New methods and datasets based on 'urban ecoregions'. Remote Sensing of Environment, 114, 1733–1746.

SDGs (2020). Goal 11 .:. Sustainable Development Knowledge Platform. https://sustainabledevelopment.un.org/sdg11.

Shi, L., Taubenböck, H., Zhang, Z., Liu, F., & Wurm, M. (2019). Urbanization in China from the end of 1980s until 2010 – spatial dynamics and patterns of growth using EO-data. International Journal of Digital Earth, 12, 78–94.

Summers, T. (2016). China's 'New Silk Roads': sub-national regions and networks of global political economy. Third World Quarterly, 37, 1628–1643.

Suprabha Baniya, Nadia Rocha, & Michele Ruta (2019). Trade Effects of the New Silk Road ,A Gravity Analysis.

Taubenböck, H., Wiesner, M., Felbier, A., Marconcini, M., Esch, T. & Dech, S. (2014). New dimensions of urban landscapes: The spatio-temporal evolution from a polynuclei area to a mega-region based on remote sensing data. Applied Geography. vol. 47, pp. 137-153.

Taubenböck, H., Esch, T., Felbier, A., Wiesner, M., Roth, A., & Dech, S. (2012). Monitoring urbanization in mega cities from space. Remote Sensing of Environment, 117, 162–176.

Taubenböck, H., Wegmann, M., Roth, A., Mehl, H., & Dech, S. (2009). Urbanization in India – Spatiotemporal analysis using remote sensing data. Computers, Environment and Urban Systems, 33, 179–188.

Taubenböck, H., Weigand, M., Esch, T., Staab, J., Wurm, M., Mast, J., & Dech, S. (2019). A new ranking of the world's largest cities–Do administrative units obscure morphological realities? Remote Sensing of Environment, 232, 111353.

United Nations (2019). Department of Economic and Social Affairs, Population Division.World Population Prospects 2019: Data Booket. ST/ESA/SER. A/424.

Verma, D., Jana, A., & Ramamritham, K. (2018). Classification of the structure of cities through mid-resolution satellite imagery and patch based neural networks. ISPRS - International Archives of the Photogrammetry, Remote Sensing and Spatial Information Sciences, XLII-5, 713–717.

Wang, H., Ning, X., Zhang, H., Liu, Y., & Yu, F. (2018). Urban boundary extraction and urban sprawö measurement using high-resolution remote sensing images: A case study of China's provincial. ISPRS - International Archives of the Photogrammetry, Remote Sensing and Spatial Information Sciences, XLII-3, 1713–1719.

Wang, Y. (2016). Offensive for defensive: the belt and road initiative and China's new grand strategy. The Pacific Review, 29, 455–463.

Xue, X., Yu, Z., Zhu, S., Zheng, Q., Weston, M., Wang, K., Gan, M., & Xu, H. (2018). Delineating Urban Boundaries Using Landsat 8 Multispectral Data and VIIRS Nighttime Light Data. Remote Sensing, 10, 799.

ISBN 978-3-9504945-0-1. Editors: M. SCHRENK, V. V: POPOVICH, P. ZEILE, P. ELISEI, C.BEYER, J. RYSER, G. STÖGLEHNER